

Two-Dimensional Classical Anisotropic Heisenberg Ferromagnets*

J. D. Patterson[†] and G. L. Jones

Department of Physics University of Notre Dame, Notre Dame, Indiana 46556

(Received 14 August 1970)

Modified Monte Carlo calculations are presented for a finite two-dimensional lattice of classical spins coupled by anisotropic Heisenberg exchange interactions. Most of the arrays considered had $N=100$ spins. The most extensive calculations were done for the zero-field magnetization and energy as a function of temperature for an anisotropy halfway between the isotropic Heisenberg and the Ising limits. The effects of adding a field and of varying the anisotropy were considered. Limited calculations of the constant-temperature magnetic susceptibility and the constant-field specific heat were also attempted. The available high-temperature power series for the isotropic zero-field Heisenberg case for infinite N was calculated for use as a check on the Monte Carlo calculations. Lowest-order spin-wave theory, as a function of anisotropy and field, was developed explicitly for the infinite N low-temperature case. As might be expected, the agreement of spin-wave theory with the Monte Carlo results improves with increasing anisotropy and field. The fairly good agreement at high temperatures that we get between the series and the Monte Carlo calculations shows that a large lattice is not needed to represent an infinite lattice in this temperature region. The fairly good agreement (especially for the mean energy) that we obtain between the Monte Carlo technique and the spin-wave theory indicates that a large lattice is not needed to approximate an infinite lattice at low temperatures as long as the anisotropy and/or field is fairly large. Owing to limited computer time, we were not able to make our method converge near the critical temperature, or below the critical temperature when the anisotropy and field were very small. Finally, we only saw evidence for one critical temperature, and its value appears to be somewhat larger than but of the same order of magnitude as the Stanley-Kaplan transition temperature.

I. INTRODUCTION

The motivation of this work resides in the fact that actual crystals exist which show two-dimensional behavior (as discussed in Sec. II) and in the fact that several interesting theoretical results are associated with the coupling of spins in two-dimensional arrays (as discussed in Sec. III).

As has been mentioned by many others, Monte Carlo methods can provide "experimental results" for theoretical calculations and "theoretical results" for experiments. Within the assumptions of the model studied (the main one being that we are limited to finite arrays of classical spins), the Monte Carlo method provides a straightforward way of obtaining results whose accuracy is limited only by the availability of computer time. As faster computers are built, the Monte Carlo method will surely increase in importance.

In Sec. IV we choose a simple model of two-dimensional spins in which the spins are on a square lattice and have only nearest-neighbor ferromagnetic coupling. In Sec. V we discuss the most familiar analytical techniques that can be used to calculate magnetic properties at high temperatures (series) and at low temperatures (spin waves). In Sec. VI we present the results of our Monte Carlo series and spin-wave calculations. Finally, in Sec. VII we present the conclusions of this study.

II. ACTUAL CRYSTALS

In order for actual three-dimensional crystals to show two-dimensional magnetic behavior it is necessary that they have a set of parallel planes in which there is strong intraplanar coupling between magnetic moments, but negligible (for many pur-

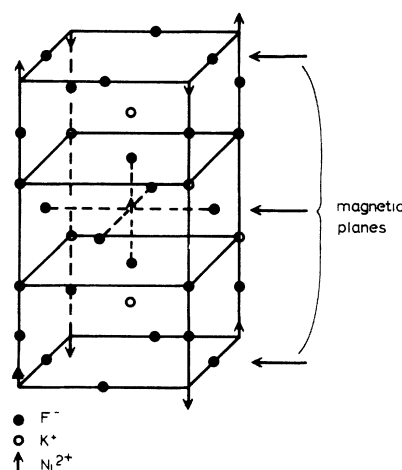


FIG. 1. Crystal structure of K_2NiF_4 , $T_N=97.1^\circ K$. Ni^{2+} carries the magnetic moment and hence determines the "magnetic planes."

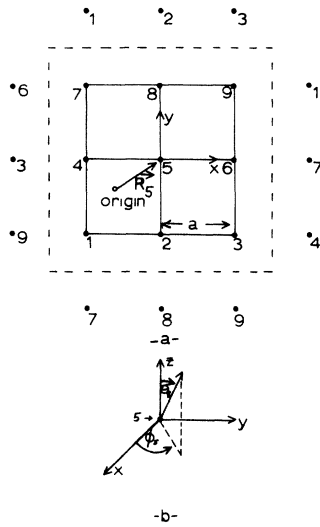


FIG. 2. Notation for square array of spins. (a) Illustration with example of special periodic boundary conditions that were used. (b) Definition of angles used at each site.

poses) interplanar coupling. The best evidence for two-dimensional coupling of the magnetic moments comes from neutron scattering.¹

Perhaps the most familiar crystal that shows two-dimensional magnetic ordering is K_2NiF_4 .¹ Its structure is shown in Fig. 1. This crystal has antiferromagnetic ordering as do many of the crystals which show predominant two-dimensional magnetic ordering. The Néel temperature for K_2NiF_4 is $T_n = 97.1^\circ$.¹ Figure 1 shows long-range order in three dimensions as well as two. Lines has shown² for a magnetic structure such as K_2NiF_4 that interplanar exchange (between neighboring magnetic planes) of either sign actually works to oppose long-range order in the direction perpendicular to the set of planes. However, once the spins are ordered relative to the given set of planes, very weak interplanar exchange between next-nearest-neighbor

TABLE I. Coefficients used for an approximate evaluation of the complete elliptic integral. More decimal places are listed in the original reference than we found necessary to use.

l	a_l	b_l
1	1.386 294 361	0.5
2	0.096 663 443	0.124 985 936
3	0.035 900 924	0.068 802 486
4	0.037 425 637	0.033 283 553
5	0.014 511 962	0.004 417 870

TABLE II. Coefficients in the susceptibility χ_T and (nn) correlation functions $\langle \tilde{S}_0 \cdot \tilde{S}_1 \rangle$ for the square lattice (Ref. 15).

l	a_l	c_l
1	2.6667	0.6667
2	5.3333	0
3	9.9556	0.414 82
4	16.9086	0
5	27.2404	-0.052 67
6	42.2122	
7	63.0670	
8	91.6638	
9	129.4967	

magnetic planes as well as other weak effects² may work to produce long-range order in the direction perpendicular to the planes. If all coupling between layers were negligible, then any plane of spins could be turned upside down in Fig. 1, with no resulting change in energy. If there were some slight coupling between next-nearest-neighbor planes in Fig. 1, but no other coupling, then all spins in half of the planes (each plane separated by two interplanar distances) could be turned upside down with no change in energy. The present evidence suggests that K_2NiF_4 is describable by a Heisenberg-Hamiltonian with only weak anisotropy.³

Similar examples of other two-dimensional magnetic crystals are K_2MnF_4 , Rb_2MnF_4 , Rb_2FeF_4 , and Ca_2MnO_4 .⁴ They all have the same crystal structure as K_2NiF_4 , but they may show different magnetic ordering due to differing coupling strengths. Crystals with the same crystal structure as K_2NiF_4 may have such highly anisotropic coupling that they are better described by an Ising model.⁵ Examples are K_2CoF_4 and Rb_2CoF_4 .

Ba_2NiF_6 and related crystals form another set of two-dimensional magnetic systems.⁶ Some two-dimensional magnetic crystals such as Di-p-Anisyl nitrosyl,⁷ $Cu(HCOO)_2 \cdot 4H_2O$,⁸ and $Mn(HCOO)_2 \cdot 2H_2O$ ⁹ have very complex crystal structures. There are even examples of two-dimensional magnetic crystals which apparently order ferromagnetically. Examples are $Cu(CH_3NH_3)_2Cl_4$ and $Cu(C_2H_5NH_3)_2Cl_4$. More examples of two-dimensional magnetic systems such as $MnTiO_3$ ¹⁰ are being discovered.

The existence in nature of two-dimensional magnetic ordering gives some motivation for its study. Whether or not useful practical applications will be found for these crystals appears to be an open question.

III. SUMMARY OF SOME KNOWN THEORETICAL RESULTS

The study of two-dimensional magnets is not only motivated by their existence but also by several in-

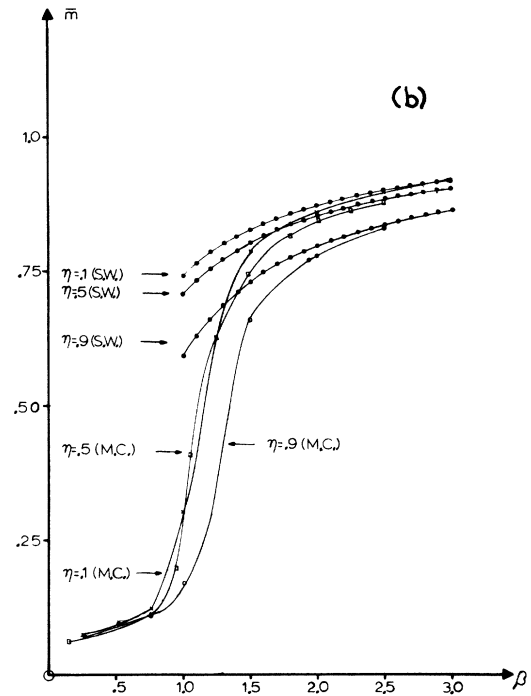
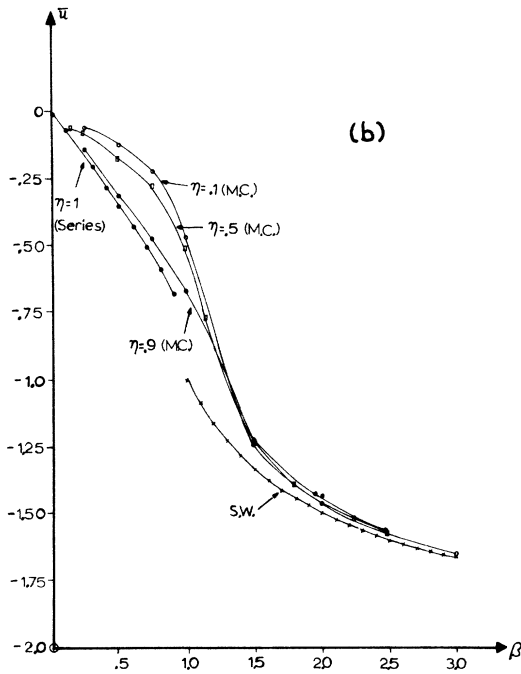
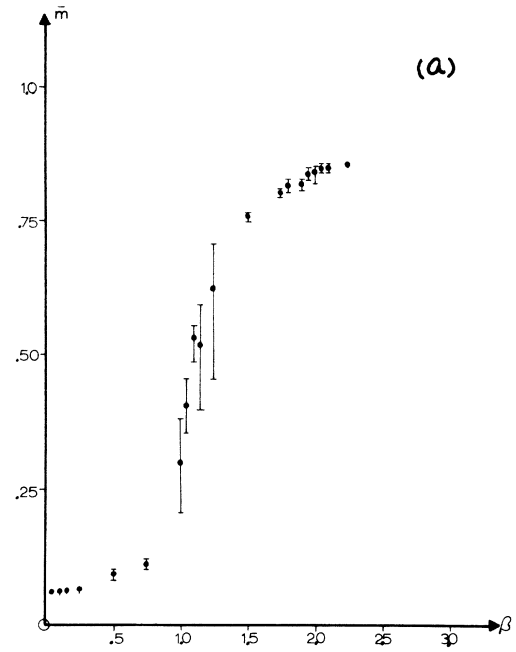
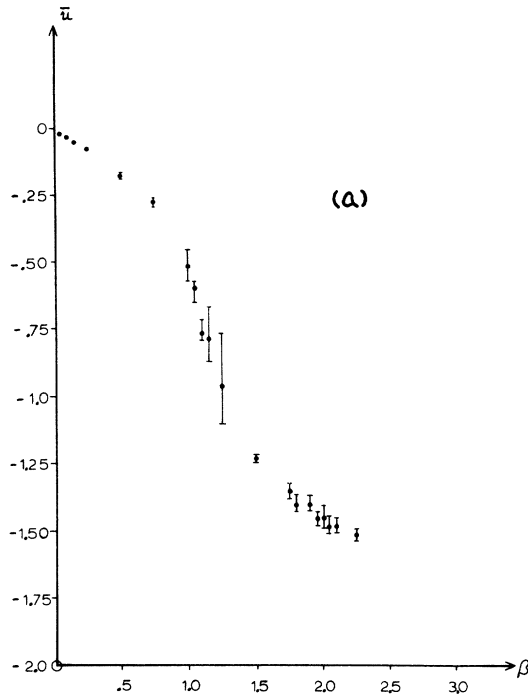


FIG. 3. Mean energy (\bar{u}) vs β by Monte Carlo calculations for $h=0$ and $N=100$. (a) Results, with "error bars," for the $\eta=0.5$ case. (b) Results for $\eta=0.1, 0.5$, and 0.9 compared to spin-wave calculations (independent of anisotropy) at low temperatures, and series results (for $\eta=1$) at high temperatures.

FIG. 4. rms magnetization (\bar{m}) vs β by Monte Carlo calculations for $h=0$ and $N=100$. (a) Results, with "error bars," for the $\eta=0.5$ case. (b) Results for $\eta=0.1, 0.5$, and 0.9 compared to spin-wave calculations at low temperatures.

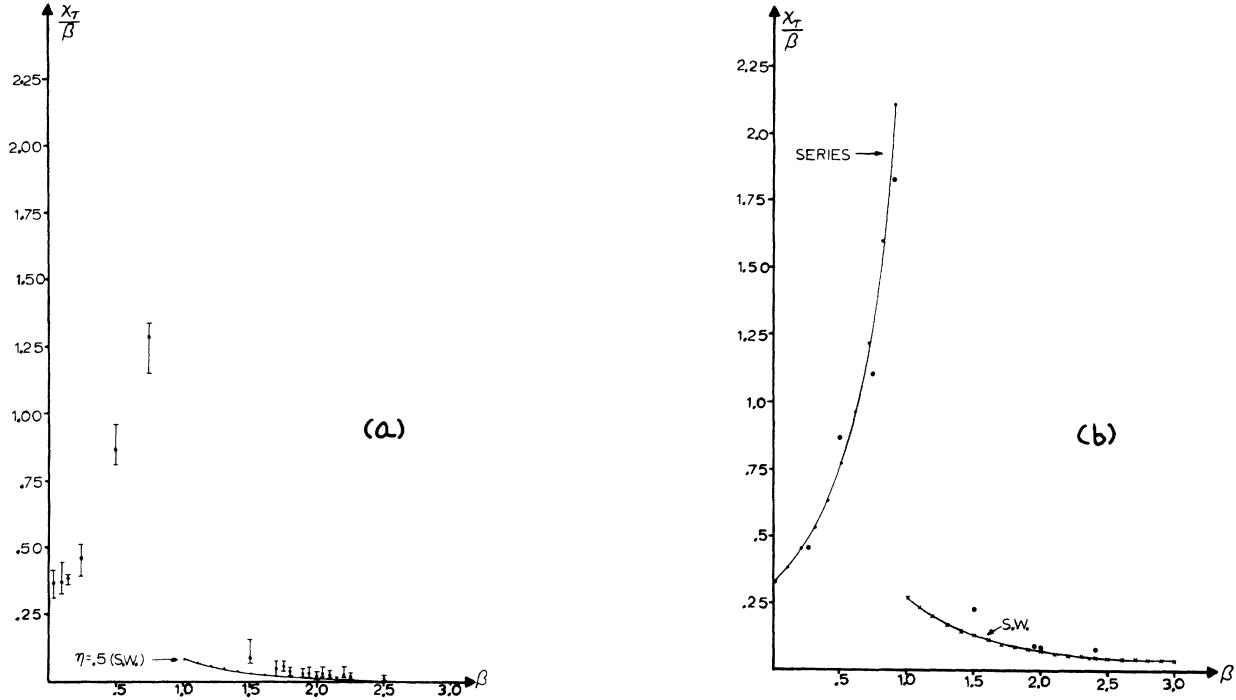


FIG. 5. Susceptibility (χ_T/β) vs β by Monte Carlo calculations for $h = 0$ and $N=100$. (a) Results, with "error bars" for the $\eta=0.5$ case. Spin-wave results are shown for comparison at low temperatures. Several Monte Carlo results from $\beta=1.0$ to 1.25 have been omitted because they show too much fluctuation to permit a clear plot. The susceptibility is very large in this region, however. (b) χ_T/β vs β for the $\eta=1$ series at high temperature and for the $\eta=0.9$ spin-wave results at low temperature. Some $\eta=0.9$ Monte Carlo calculations (black dots) are shown for comparison.

interesting theoretical questions which surround them. Only results for Heisenberg (isotropic and anisotropic) magnetic systems will be considered here as most actual crystals seem to fit this category.

A. Rigorous Results for the Isotropic Case

For nearest-neighbor (or at least suitably restricted finite-range) ferromagnetic exchange interactions, Mermin and Wagner¹¹ have shown that the intensive magnetization $\langle m_z \rangle$ (for magnetic fields h in the z direction) satisfies the inequality

$$\langle m_z \rangle_{N=\infty} \cong (\text{const}/\sqrt{T})(1/|\ln|h||)^{1/2} \rightarrow 0 \text{ as } h \rightarrow 0, \quad (1)$$

where T is the temperature and N is the number of spins in a two-dimensional lattice. Jasnow and Fisher¹² have proved a similar theorem without the necessity of introducing a symmetry breaking field. Their result is equivalent to the following result:

$$\langle m_z^2 \rangle_{h=0} \cong (\text{const}/T)(1/\ln N) \rightarrow 0 \text{ as } N \rightarrow \infty. \quad (2)$$

Both of these results show that two-dimensional isotropic Heisenberg systems do not show spontaneous ferromagnetization. Spontaneous antiferro-

magnetism has also been ruled out by Mermin and Wagner.¹¹ Arbitrary types of magnetic order have not been ruled out, but it would seem (in view of these theorems) that the burden of proof rests on proving their existence (rather than their lack of existence) in two-dimensional systems.

The physical reason for the lack of spontaneous magnetization in two-dimensional Heisenberg ferromagnets apparently resides in the density of states of the low-energy spin-wave excitations in these systems.⁶ If $D(E)$ denotes this density of states, for small energies (E) in the isotropic Heisenberg systems we have

$$D_{2D}(E) \propto \text{const} \quad (3a)$$

and

$$D_{3D}(E) \propto \sqrt{E}. \quad (3b)$$

Thus, low-lying energy excitations are more important in two dimensions than in three. In two dimensions, the Mermin-Wagner theorem tells us that the ordered ground state is unstable with respect to thermal excitations at any nonzero temperature, no matter how small. The connection of the Mermin-Wagner theorem with the density of states will be made clearer later within the context of spin-

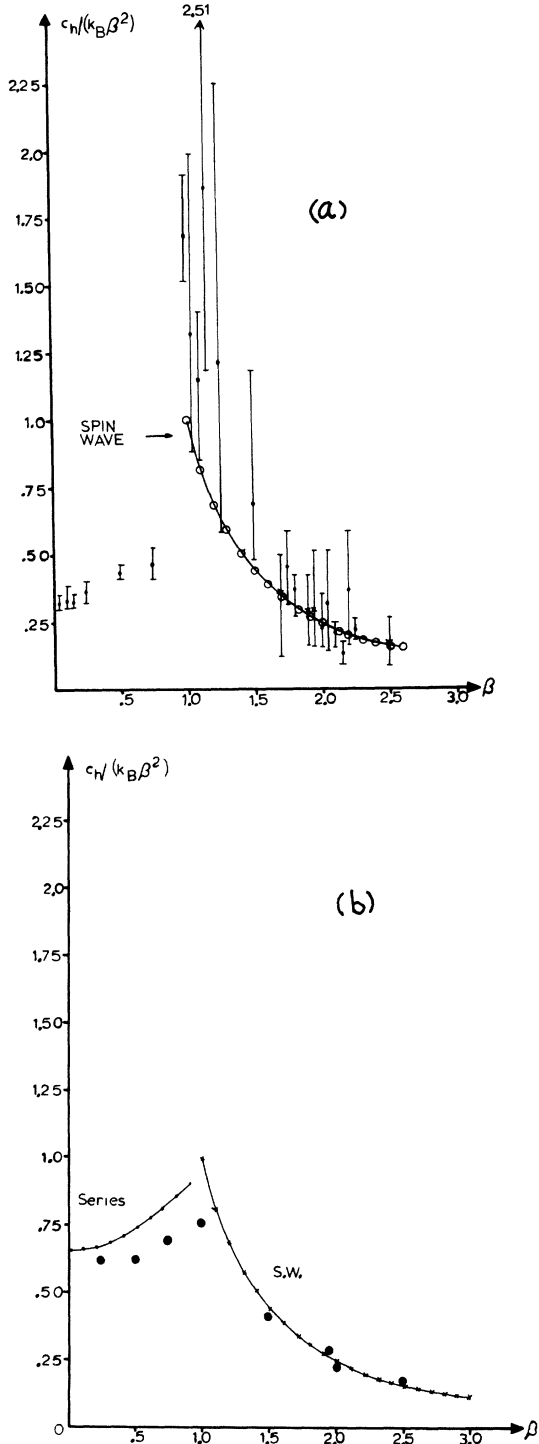


FIG. 6. Specific heat [$c_H/(k_B\beta^2)$] vs β by Monte Carlo calculations for $h=0$ and $N=100$. (a) Results, with "error bars" for the $\eta=0.5$ case. Spin-wave results are shown for comparison at low temperature. (b) $c_H/(k_B\beta^2)$ vs β for the $\eta=1$ series at high temperature and for the spin-wave results (independent of anisotropy) at low temperature. Monte Carlo calculations (black dots) are shown for comparison for $\eta=0.9$.

wave theory.

For the Heisenberg model with general anisotropy there are no results which are both rigorous and of great use. However, the Mermin-Wagner theorem does not forbid spontaneous magnetization for this case. Thus, we may expect that suitable anisotropy will support long-range order in two dimensions.

B. Calculational Results ($N = \infty$)

We first consider the anisotropic case at low temperature. For this situation spin-wave theory can be used to derive useful results. Only the classical ferromagnetic case will be considered both here and in our computer calculations. The basic assumptions of spin-wave theory are that (i) there exists an ordered ground state (which is assumed to be characterized by a magnetization in the z direction), and (ii) the deviations from the ordered ground state are small. We characterize this by saying $S_x \ll S$, $S_y \ll S$, and $S - S_z \ll S$, where S_x , S_y , and S_z are the components of the classical spin S in the x , y , z directions.

In order to make direct comparisons with our calculations we will discuss spin-wave theory in more detail later. As we will see, for low temperatures and in lowest order, spin-wave theory predicts (in suitable units)

$$\langle m_z \rangle = S - (a/2\pi)^2 \int_{\text{BZ}} (k_B T / \omega_k) d^2k, \quad (4)$$

where a is the lattice spacing of an (assumed) square lattice k_B is Boltzmann's constant, BZ refers to the first Brillouin zone, and ω_k gives the relation between the frequency and wave vector of the spin waves. For small k , we will find that

$$\omega_k = a'k^2 + b(h, \text{anisotropy}), \quad (5)$$

where a' is a constant, and the function b vanishes in zero field with no anisotropy. Equation (4) therefore diverges if $b=0$. This is interpreted as meaning that an ordered ground state is impossible. The Mermin-Wagner theorem, of course, supports this conclusion.

It is perhaps still not entirely clear how valid the ($b \neq 0$) spin-wave results are; however, experimental results suggest that they may be very good at low temperatures.¹³ In any case, spin-wave theory predicts that the magnetization is rather sensitive to small amounts of anisotropy, and this assumption is borne out by more extensive Green's-function calculations.^{4, 14}

Results are also available for the zero-field isotropic case at high temperature. These results are derived from expansion of quantities derived from the partition function in powers of the reciprocal temperature. Particularly interesting is the zero-field susceptibility

$$\chi = \sum_0^\infty a_i (J/k_B T)^i, \quad (6)$$

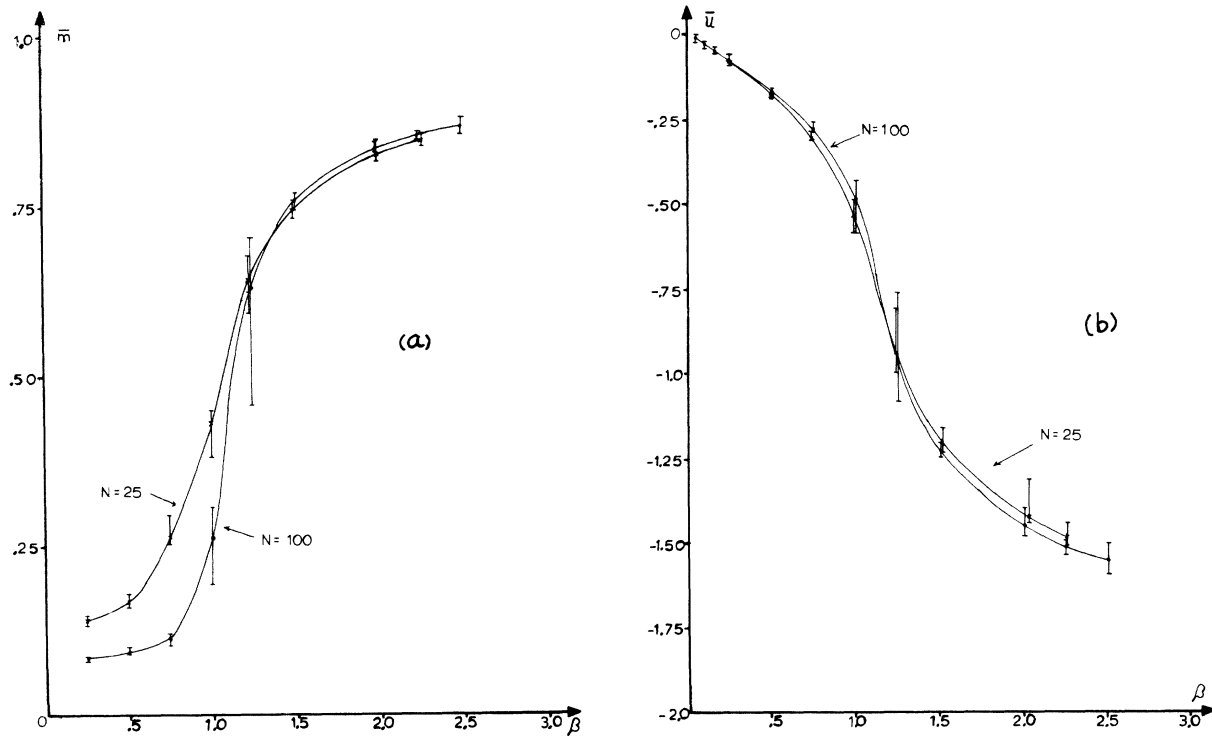


FIG. 7. (a) rms Monte Carlo magnetization (\bar{m}) vs β for $h=0$, $\eta=0.5$, and $N=25$ and 100. (b) Monte Carlo mean energy (\bar{u}) vs β for $h=0$, $\eta=0.5$, and $N=25$ and 100.

where J is the exchange constant measuring the strength of nearest-neighbor coupling (we will restrict ourselves to this case). By use of "diagram counting," the a_l have been exactly evaluated up to $l=9$ ¹⁵ for classical spins. Although they are non-rigorous, Padé approximants have in the past proved to be a reliable method of extrapolating such series into the neighborhood of the critical temperature. Stanley and Kaplan¹⁶ have used such a technique for two-dimensional lattices. They found $\chi^{-1} \rightarrow 0$ at $T \equiv T_c^{(2)} > 0$ (in our units with $J=S=1$, Stanley's¹⁵ results give for the square lattice of classical spins $\beta_c^{(2)} = 1/k_B T_c^{(2)} \cong 2.31$). If the susceptibility really diverges without the appearance of spontaneous magnetization, then these isotropic two-dimensional systems appear to show a new type of phase transition. Independent work by Moore¹⁷ tends to confirm the Stanley-Kaplan transition.

The Stanley-Kaplan transition implies further results.¹⁶ If S_{iz} labels the z component of spin at site \vec{R}_i , then $S_{iz} = S \cos \theta_i$, where θ_i measures the angle of inclination of \vec{S}_i relative to the z axis. It is then easy to show (directly, or as a consequence of the fluctuation-dissipation theorem) that the magnetic susceptibility at constant temperature parallel to the z axis χ_T can be written

$$\chi_T = \beta S^2 \sum_i \langle \cos \theta_i \cos \theta_0 \rangle \quad (7)$$

where $\beta = (k_B T)^{-1}$ and $\langle \dots \rangle$ means a statistical average. In (7) the sum over i runs over the whole lattice. Normally, an equation such as (7) is only appropriate in the paramagnetic region, but for our two-dimensional isotropic Heisenberg lattice, the magnetization vanishes at all temperatures and so Eq. (7) is valid for all temperatures. If we suppose for large $|\vec{R}_i - \vec{R}_0|$ that $\langle \cos \theta_i \cos \theta_0 \rangle \sim |\vec{R}_i - \vec{R}_0|^{-\lambda}$, then the Stanley-Kaplan result indicates $\lambda \leq 2$ (as $T \rightarrow T_c^{(2)+}$). On the other hand, the requirement of no spontaneous magnetization says $\lambda > 0$. It probably would be unreasonable to suppose that $\langle \cos \theta_i \cos \theta_0 \rangle$ decreases as T is lowered below $T_c^{(2)}$. Thus, if we believe the Stanley-Kaplan result, we almost have to believe that the magnetic susceptibility diverges for all $T < T_c^{(2)}$.

We would expect that χ would not be very sensitive to small amounts of anisotropy for $T \gg T_c^{(2)}$, but perhaps very sensitive to small amounts of anisotropy (the causative factor of spontaneous magnetization) at low temperatures. The limit of complete isotropy may be a special case. Three-dimensional calculations have indicated that the critical exponents characterizing magnetic behavior near T_c may

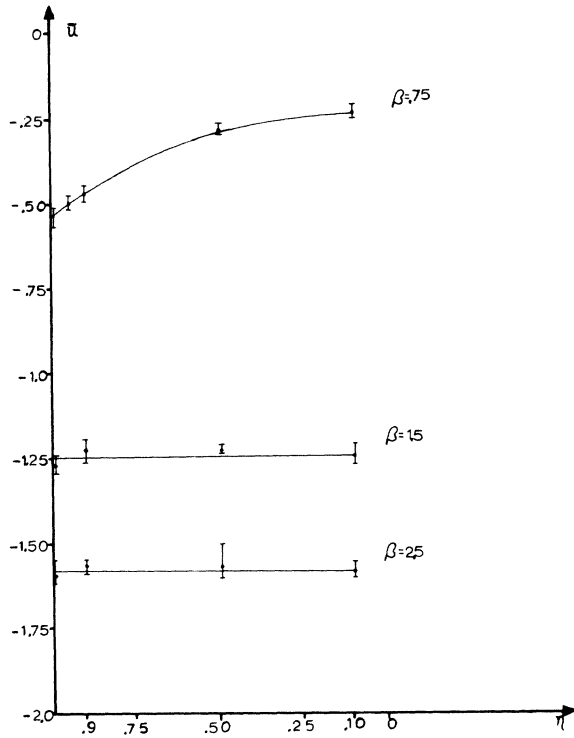


FIG. 8. Monte Carlo mean energy (\bar{u}) vs η for $h=0$, $N=100$, and $\beta=0.75, 1.5$, and 2.5 . Only at $\beta=0.75$ does there appear to be any evidence for variation of \bar{u} with η .

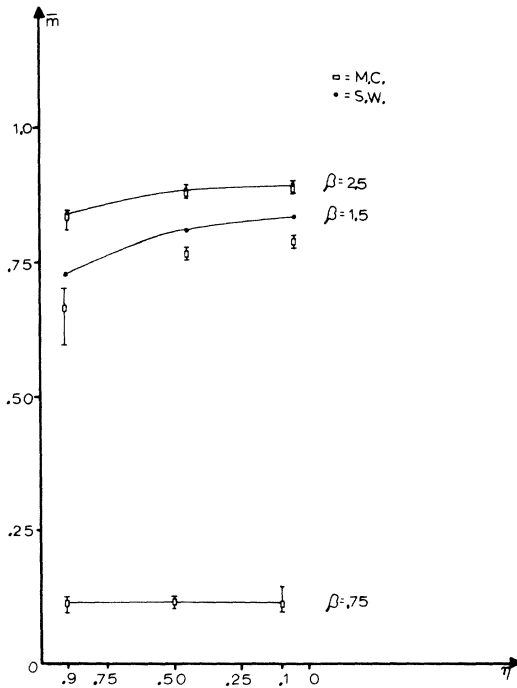


FIG. 9. rms Monte Carlo magnetization (\bar{m}) vs η for $h=0$, $N=100$, and $\beta=0.75, 1.5$, and 2.5 . Spin-wave results for $\beta=1.5$ and 2.5 are shown for comparison.

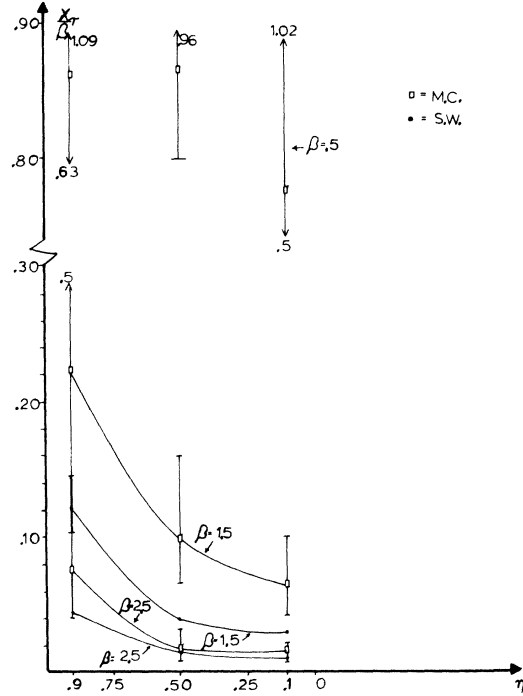


FIG. 10. χ_T/β vs η by Monte Carlo calculations for $h=0$, $N=100$, and $\beta=0.5, 1.5$, and 2.5 . The $\beta=0.5$ results show too much fluctuation to be very meaningful. Shown for comparison are the spin-wave results for $\beta=1.5$ and 2.5 .

change abruptly as the anisotropy vanishes.¹⁸

Known results on two-dimensional magnets thus raise the following questions:

(a) Do we really have a transition of the Stanley-Kaplan type? There appears to be no hard experimental evidence to establish its existence.

(b) If a Stanley-Kaplan transition exists, does it (or its analog) continue to exist in the presence of small amounts of anisotropy?

(c) It appears to be generally accepted that small amounts of appropriate anisotropy will cause the appearance of spontaneous magnetization at some temperature > 0 (say $T_c^{(1)}$). If the Stanley-Kaplan transition persists for small amounts of anisotropy, we wonder if there is a relation between $T_c^{(1)}$ and $T_c^{(2)}$. In particular, we would like to know whether or not they are equal. A particularly intriguing Green's-function calculation by Lines indicates that they may be equal.¹⁴

(d) What magnetic properties (if any) change abruptly as isotropy is approached? For what temperatures or temperature ranges are these changes important?

(e) For the isotropic case (for which the magnetization vanishes) is χ_T infinite for all $T < T_c^{(2)}$? Besides arguments already given, the calculation

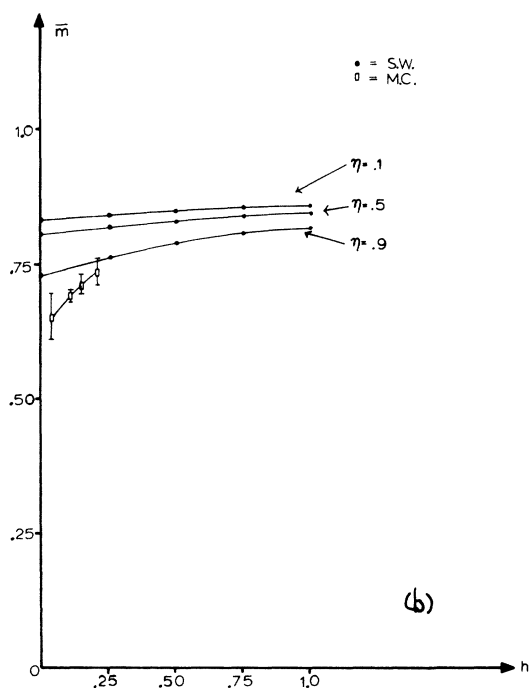
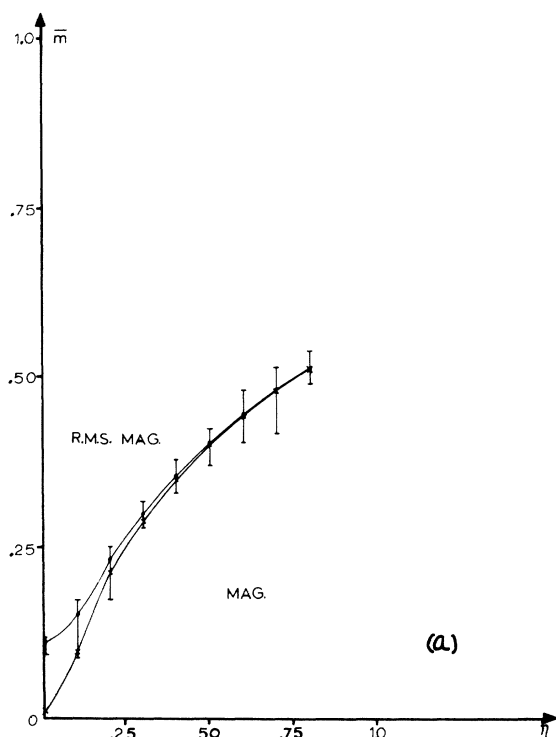


FIG. 11. Magnetization (\bar{m}) vs field (h) for $N=100$. (a) Monte Carlo magnetization and rms magnetization vs h for $\eta=0.9$ and $\beta=0.75$. (b) Spin-wave magnetization vs h for $\beta=1.5$ and $\eta=0.1, 0.5$, and 0.9 . A few Monte Carlo (rms) results are shown for small h for the $\eta=0.9$ case (where the deviation from the spin-wave results should be greatest).

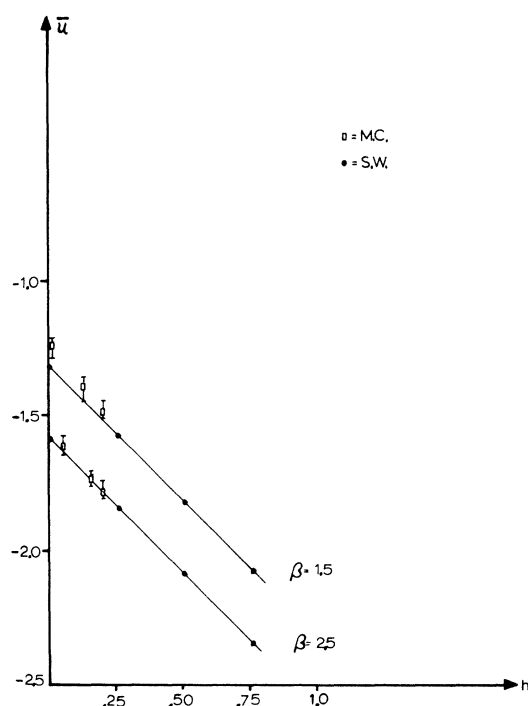


FIG. 12. Mean energy (\bar{u}) vs h for $N=100$, $\eta=0.9$, and $\beta=1.5$ and 2.5 . Monte Carlo results are only given for weak fields where the deviation from the spin-wave results should be the greatest. The spin-wave results are independent of anisotropy.

by Lines¹⁴ would seem to indicate that it is and further that χ_T is very large even with small anisotropy unless the temperature is very small.

(f) We know that two-dimensional systems have extended short-range order and critical fluctuations (of a quantity from its mean value).⁴ We would like to know more about the various effects that these can cause. In particular, paramagnons about T_c and zero-point deviations (for nonclassical antiferromagnets) appear to be uniquely important for two-dimensional systems.

IV. MODEL STUDIED

Before we become more explicit about the results of spin-wave theory, series, and our own calculations, it is necessary to explicitly define the model studied. In defining our model it is useful to list the ways it differs from actual two-dimensional crystals. The *approximations* we make consist in ignoring such differences. We also list specific *assumptions* made to define the model. The assumptions may be valid for some real two-dimensional magnetic systems. The distinction between *assumptions* and *approximations* is probably not always clear cut, but it does provide a convenient way to characterize the model studied.

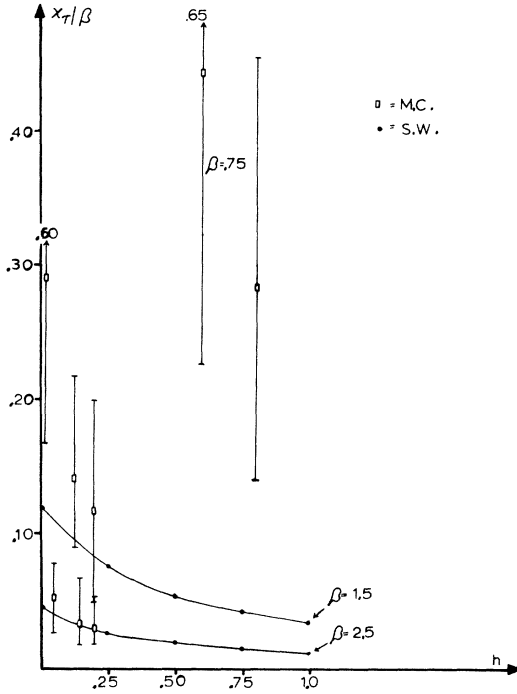


FIG. 13. χ_T/β vs h for $N=100$, $\eta=0.9$, and $\beta=0.75$, 1.5, and 2.5. The Monte Carlo results show too much fluctuation to be very meaningful for the $\beta=0.75$ case. Spin-wave results are shown for comparison at $\beta=1.5$ and 2.5. The agreement between spin-wave and Monte Carlo results gets worse for higher temperatures and weaker fields.

Approximations. (i) The crystal is small; (ii) the spins are classical, that is, they have finite length but no space quantization; (iii) the coupling between spins is strictly zero in directions perpendicular to the planes of strongly coupled spins; (iv) lattice vibrations can be ignored; (v) secondary effects such as magnetostriction are of no importance; and (vi) a special kind of periodic boundary condition as defined in Fig. 2 can be used.

Assumptions. (a) The anisotropic Heisenberg model provides a valid description; This means that not all conceivable types of anisotropy are considered; (b) the coupling between spins is of such a sign as to favor ferromagnetic alignment; (c) only one domain need be considered when we have spontaneous magnetization. More generally, we assume the average of the total magnetization gives a true measure of long-range order; (d) no demagnetization fields need be considered; (e) there is only one kind of spin, so $|\vec{S}_i|=S$ for all sites labeled by i ; (f) the spins are arranged on a square array; and (g) only nearest-neighbor coupling between spins will be considered.

The notation for the square array of N spins is defined by Fig. 2. The case $N=9$ is shown. The

boundary conditions are indicated by the numbers outside the square. This particular choice of boundary conditions facilitates programming our problem because the nearest neighbors of site i are at $i \pm 1 \pmod{N}$ and $i \pm \sqrt{N} \pmod{N}$ for all i whether or not i is on the boundary.¹⁹ The choice of location of the origin for the vectors \vec{R}_i specifying the sites is, of course, arbitrary.

In the Heisenberg model, we assume that the coupling between the spins and the coupling of the spins with an external field h (in the z direction) can be represented in suitable units by the following Hamiltonian:

$$H = -S^2 \sum_{i,j=1}^N [J_x(\vec{R}_i - \vec{R}_j) \sin\theta_i \cos\phi_i \sin\theta_j \cos\phi_j + J_y(\vec{R}_i - \vec{R}_j) \sin\theta_i \sin\phi_i \sin\theta_j \sin\phi_j + J_z(\vec{R}_i - \vec{R}_j) \cos\theta_i \cos\theta_j] - Sh \sum_{i=1}^N \cos\theta_i. \quad (8)$$

As already mentioned, we assume the J 's connect only nearest neighbors (nn) and that all J 's > 0 . We wish there to be no self-coupling of the spins so we must assume $J_x(0) = J_y(0) = J_z(0) = 0$. We assume (by symmetry) that all J_x for nn are the same, and similarly for J_y and J_z . The isotropic case is defined by $J_x = J_y = J_z$, otherwise we have anisotropy. In the extreme anisotropic model we have an Ising model ($J_x = J_y = 0$, $J_z \neq 0$).

The average instantaneous magnetic moment along the field is represented by

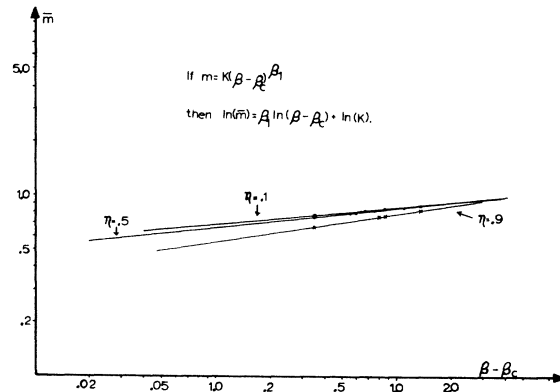


FIG. 14. Log-log plot of Monte Carlo magnetization (\bar{m}) vs $\beta - \beta_c$ for $h=0$, $N=100$, and $\eta=0.1$, 0.5, and 0.9. β_c was chosen to be 1.15. It is possible to make the lines parallel by assuming a large variation of β_c with η . For example, the ($\eta=0.1$, $\beta_c=0.9$) and ($\eta=0.9$, $\beta_c=1.3$) lines are almost parallel. The slope of the $\eta=0.5$ line is about 0.11 compared to the slope expected for a pure Ising system of 0.125.

$$m_z = (S/N) \sum_{i=1}^N \cos \theta_i . \quad (9)$$

We are more interested in statistical averages than dynamical quantities because they represent directly measurable thermodynamic quantities. Using a canonical ensemble, the statistical averages are defined in the usual way,

$$\langle f \rangle = \frac{\int e^{-\beta H} f(\dots, \theta_i, \phi_i, \dots) d\Gamma}{\int e^{-\beta H} d\Gamma} , \quad (10)$$

where

$$d\Gamma = \prod_{i=1}^N d\mu_i , \quad d\mu_i = \sin \theta_i d\theta_i d\phi_i , \quad 0 \leq \theta_i < \pi , \quad 0 \leq \phi_i < 2\pi .$$

By inspection (and some manipulation for the last two cases) we can easily write the following static properties in terms of statistical averages as shown:

$$\text{mean energy} = \bar{u} = (1/N) \langle H \rangle , \quad (11)$$

$$\text{magnetization} = \bar{m} = \langle m_z \rangle , \quad (12)$$

specific heat at

$$\begin{aligned} \text{constant field} &= c_h = (1/N) (\partial \langle H \rangle / \partial T) \\ &= (k_B \beta^2 / N) (\langle H^2 \rangle - \langle H \rangle^2) , \end{aligned} \quad (13)$$

parallel susceptibility at

$$\begin{aligned} \text{constant temperature} &= \chi_T = \partial \langle m_z \rangle / \partial h \\ &= N \beta (\langle m_z^2 \rangle - \langle m_z \rangle^2) . \end{aligned} \quad (14)$$

For interesting cases, we cannot evaluate these expressions exactly in closed form, so resort to some form of approximation is necessary. We first discuss in more detail the analytical approximations at low temperatures (spin waves) and at high temperatures (series expansions) and then proceed to discuss the numerical calculations. The analytical techniques assume $N = \infty$, whereas most of our numerical calculations did not go beyond $N = 100$. By comparing the two we should get some feeling for the importance of restricting the lattice to a small size.

V. APPLICABLE ANALYTICAL TECHNIQUES AT HIGH AND LOW TEMPERATURES

A. Spin-Wave Theory

Let us choose $J_x = J_y = \eta$, $S = 1$, and $J_z = 1$. Then we can write our Hamiltonian as

$$\begin{aligned} H &= -\frac{1}{2} \sum_{\substack{i,j=1 \\ (\text{nn})}}^N \vec{S}_i \cdot \vec{S}_j \\ &+ \frac{1}{2} \sum_{\substack{i,j=1 \\ (\text{nn})}}^N (1-\eta) (S_{ix} S_{jx} + S_{iy} S_{jy}) - h \sum_{i=1}^N S_{zi} , \end{aligned} \quad (15)$$

where the factor of $\frac{1}{2}$ is inserted so that each bond is weighted only once [alternatively, we could let the sum over i and j in Eq. (8) count each pair $i-j$ twice, as it does in Eq. (15), and then choose $J_x = \frac{1}{2}$, and $\eta = 2J_x = 2J_y$]. Using standard techniques^{19,20} the Hamiltonian immediately generates a set of dynamical equations for the spins. We then can make the usual spin-wave approximation which consists of neglecting terms of order $S_i S_j$ and replacing S_j by 1 in the dynamical equations. By Fourier transforming this set of equations one readily finds that the normal mode frequencies (for each wave vector \vec{k}) for a square lattice are given by

$$\omega_{\vec{k}} = h + 4 - 2\eta(\cos k_x a + \cos k_y a) . \quad (16)$$

In the long-wavelength limit Eq. (16) says

$$\omega_{\vec{k}} = h + 4(1 - \eta) + \eta a^2 k^2 , \quad (17)$$

and one gets the usual quadratic dependence on wave vector of the spin-wave frequencies (the $\omega_{\vec{k}}$). From a statistical mechanics point of view, the ideas of spin-wave theory should be valid at low temperatures. Using the long-wavelength approximation to $\omega_{\vec{k}}$ and the standard ideas of spin-wave theory,¹⁹ we obtain

$$\bar{m} = 1 - \frac{1}{\beta} \left(\frac{a}{2\pi} \right)^2 \int_0^{k_m} \frac{\pi d(k^2)}{h + 4(1 - \eta) + \eta a^2 k^2} , \quad (18)$$

where the Brillouin zone has been replaced by an equivalent circle of radius k_m defined by

$$k_m = (1/\sqrt{\pi})(2\pi/a) . \quad (19)$$

Evaluating the integrals in (18) we obtain

$$\bar{m} = 1 - \frac{1}{4\pi\eta\beta} \ln \left[1 + \frac{4\pi\eta}{h + 4(1 - \eta)} \right] . \quad (20)$$

We thus note the usual breakdown of the spin-wave theory when $\eta \rightarrow 1$ with $h = 0$ (the isotropic limit).

Further results are also readily obtained within the context of our lowest-order spin-wave approximation. The $\omega_{\vec{k}}$ cancels out of the expression for the mean energy and we find that

$$\bar{u} = -2 - h + 1/\beta . \quad (21)$$

Note that in this approximation the mean energy turns out to be independent of the anisotropy. Equation (21) does not diverge as $\eta \rightarrow 1$ and $h \rightarrow 0$. However, \bar{m} as given by Eq. (20) does. We would thus expect (for small anisotropies and fields) more trouble in calculating \bar{m} than \bar{u} . Probably the reason for this is that \bar{u} only involves terms coupling nn spins and so \bar{u} "cannot distinguish" between long-range order and long short-range order. In our computer calculations we do have more difficulty in obtaining convergent \bar{m} than in obtaining convergent \bar{u} .

The specific heat and the susceptibility are also readily evaluated in the spin-wave approximation. We have

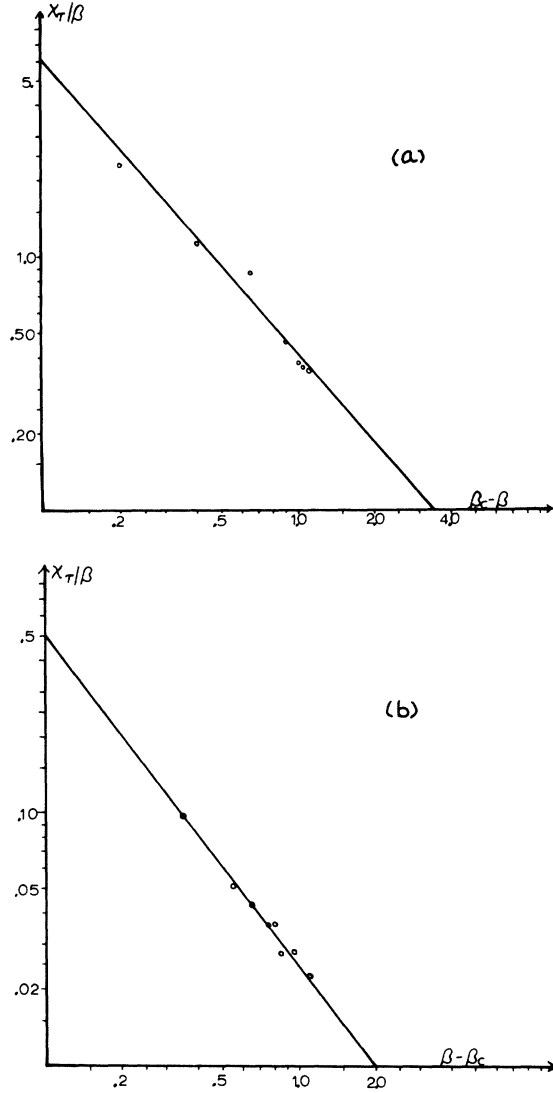


FIG. 15. Log-log plot of (χ_T/β) by Monte Carlo calculations vs $|\beta_c - \beta|$ for $\eta = 0.5$, $h = 0$, $N = 100$, and $\beta_c = 1.15$. The slopes above the critical temperature has magnitude of about 1.2. Below the critical temperature the slope has a magnitude of about 1.3. (a) $\beta < \beta_c$ ($T > T_c$); (b) $\beta > \beta_c$ ($T < T_c$).

$$\frac{c_h}{k_B \beta^2} = -\frac{\partial \bar{m}}{\partial \beta} = \frac{1}{\beta^2} \quad (22)$$

and

$$\frac{\chi_T}{\beta} = \frac{1}{\beta} \frac{\partial \bar{m}}{\partial h} = \frac{1}{[h + 4(1 - \eta)][h + 4(1 - \eta) + 4\pi\eta]} \frac{1}{\beta^2} \quad (23)$$

Equations (22) and (23) give the result

$$\frac{\chi_T}{\beta} = \frac{1}{[h + 4(1 - \eta)][h + 4(1 - \eta) + 4\pi\eta]} \frac{c_h}{k_B \beta^2}, \quad (24)$$

which says that for low temperatures, low fields,

and low anisotropy, the fluctuation in the magnetization is huge compared to the fluctuation in the energy.

For the magnetization and the susceptibility, one can do slightly better calculations than the above if one does not make the long-wavelength approximation for the spin-wave frequencies [i.e., if one uses Eq. (16) rather than Eq. (17)]. For the magnetization we obtain

$$\bar{m} = 1 - \frac{1}{\beta} \left(\frac{a}{2\pi} \right)^{\frac{1}{2}} \times \int_{-\pi/a}^{\pi/a} \int_{-\pi/a}^{\pi/a} \frac{dk_x dk_y}{h + 4 - 2\eta[\cos(k_x a) + \cos(k_y a)]}, \quad (25)$$

which, in turn, can be transformed to the form²¹

$$\bar{m} = 1 - \frac{2}{\beta\pi(h + 4)} K\left(\frac{4\eta}{h + 4}\right), \quad (26)$$

where $K(\eta_1)$ is the complete elliptic integral defined by

$$K(\eta_1) = \int_0^1 \frac{1}{[(1 - t^2)(1 - \eta_1^2 t^2)]^{1/2}} dt. \quad (27)$$

For the evaluation of Eq. (27) we have used a very accurate polynomial expression which is available.²² The expression is

$$K(\eta_1) = (a_1 + a_2\eta_2 + \dots + a_5\eta_2^4) + (b_1 + b_2\eta_2 + \dots + b_5\eta_2^4) \ln(1/\eta_2), \quad (28)$$

where $\eta_2 = 1 - \eta_1$ and the coefficients used are listed in Table I. We also have used $\chi_T = (\partial \bar{m} / \partial h)_T$, and Eqs. (26) and (28) to obtain our spin-wave values for \bar{m} and χ_T/β that we will present later.

B. High-Temperature Series

For $\eta = 1$, $h = 0$, and high temperatures, we fortunately have explicit series available to us from the work of Stanley.²³ We collect together here the needed results converted to our notation. For small η , the high-temperature results are probably not very sensitive to η .²⁴ However, differences may be noted for large (near 1) η .

The high temperature or small β expansions are immediately suggested because the canonical average contains $e^{-\beta H}$. Such expansions involve diagram counting and become impossible from a practical standpoint for all but the first few terms. Fortunately, the number of diagrams that must be counted is less for the classical case than the quantum case. For the high-temperature susceptibility, the first nine terms are available. The high-temperature susceptibility can be written (with $J = 1$)

$$\frac{\chi_T}{\chi_{\text{Curie}}} = 1 + \sum_{l=1}^{\infty} a_l \left(\frac{\beta X}{2} \right)^l, \quad (29)$$

where the first nine a_l for the square lattice are listed in Table II. In our units, $\chi_{\text{Curie}} = \frac{1}{3}\beta$. The

factor is $\frac{1}{2}\beta$ [in Eq. (29)] rather than β because we choose to count each bond of exchange coupling only once and weight it with J rather than $2J$. $X = S^2 = 1$ for our classical case. $X = S(S+1)$ if we want to compare to the quantum case. By diagram counting, we²⁵ have also worked out the first few terms for the correlation functions. The result is

$$\langle \vec{S}_0 \cdot \vec{S}_1 \rangle = X \sum_{i=1}^{\infty} c_i (\beta X/2)^i, \quad (30)$$

where again the known coefficients are listed in Table II. Since $\langle \vec{S}_0 \cdot \vec{S}_1 \rangle$ refers to nearest-neighbor correlation functions, note that

$$\bar{u} = -(1/N)^{\frac{1}{2}}(NZ) \langle \vec{S}_0 \cdot \vec{S}_1 \rangle = -2 \langle \vec{S}_0 \cdot \vec{S}_1 \rangle, \quad (31)$$

where the number of nearest neighbors is $Z = 4$. The specific heat is then given by

$$\frac{c_h}{k_B \beta^2} = +2 \frac{\partial}{\partial \beta} \langle \vec{S}_0 \cdot \vec{S}_1 \rangle. \quad (32)$$

So, high-temperature series provide a direct check on \bar{u} , c_h , and χ_T . For future purposes it is worth noting that in the limit of extremely high temperatures, only $c_1 = \frac{2}{3}$, contributes to (31) so $\bar{u} = -2 \times \frac{2}{3} \times \frac{1}{2} \beta = -\frac{2}{3} \beta$, and $c_h/(k_B \beta^2) = \frac{2}{3}$. If $\eta = \frac{1}{2}$, it can also be shown in the same limit that $c_h/(k_B \beta^2) = \frac{1}{3}$. We should also note that for the antiferromagnetic case, the series for χ_T (with suitable corrections for other effects) may provide a good fit to experimental data.²⁶ The validity of the series results can perhaps be extended to lower temperatures (but still above a critical temperature) by use of the Padé approximation technique. At these temperatures the effect of anisotropy (on say the susceptibility) probably becomes more important, and so our isotropic series would not be the right starting point for cases of interest to us.

VI. MODIFIED MONTE CARLO NUMERICAL CALCULATIONS

A. Method

Following other workers,^{19,27,28} we used a modified Monte Carlo technique to generate a canonical ensemble. For technical reasons,¹⁹ this technique appears to be limited to classical systems. The technique generates a set of M states S_i which can be shown in the limit as $M \rightarrow \infty$ to exactly represent a canonical ensemble.²⁷ For most of our calculations with $N = 100$, we chose $M \sim 10^5$, which was as large as possible for runs limited to a few minutes of UNIVAC-1107 computer time. The thermodynamic averages were computed from

$$\langle f \rangle = (1/M) \sum_{i=1}^M f(S_i). \quad (33)$$

For a given temperature, it is not entirely clear (*a priori*) what M and N must be to represent an actual crystal well. However, *a posteriori*, we can say that $N = 100$ and $M = 10^5$ certainly fail for two

cases: (i) $T \rightarrow T_c^*$ (where T_c is the analog of a true critical temperature – no true phase transition, of course, occurs for finite systems because there are no singularities in the thermodynamic functions); and (ii) $\eta \rightarrow 1$ when $T < T_c$ (the failure appears to occur only for the magnetization and susceptibility).

The first failure must be connected with the fact that the onset of critical fluctuations cause very slow convergence in representing the canonical ensemble. (Our basic criterion for convergence is repeatability of results in similar runs.) Even if we could run until convergence for finite N , we also know that the nearer we are to T_c the larger we must make N to exactly represent the critical behavior of an actual crystal (as $T \rightarrow T_c$, N must $\rightarrow \infty$). We do not understand the second failure as well. It appears that something peculiar happens when $\eta \rightarrow 1$ with $T < T_c$. If the susceptibility is really infinite (for $N = \infty$) for this case then, of course, we would expect failure. Our results are not definitive enough to make any claims. The characteristic feature of our results in this region is that the system seems to settle into metastable states of the correct energy, but the states are not necessarily representative of the magnetization. It is probable that if $\chi \rightarrow \infty$ (for $N \rightarrow \infty$) as $\eta \rightarrow 1$ and $T < T_c$, then the range over which the spins is correlated also becomes infinite, so that for our finite systems, unknown boundary effects become very important as $\eta \rightarrow 1$. Further recall that the spin-wave approximation diverges for susceptibility and magnetization but not for mean energy or specific heat.

We here summarize four arguments which favor divergent susceptibility at low temperatures for the isotropic two-dimensional Heisenberg ferromagnets. One argument is obtained from the Stanley-Kaplan result together with the belief that the correlation functions $\langle \vec{S}_i \cdot \vec{S}_0 \rangle$ increase with decreasing temperature. Spin-wave theory also predicts this divergence. The lack of convergence of our results for $T < T_c$ and $\eta \rightarrow 1$ is as mentioned consistent with $\chi \rightarrow \infty$ in this region. Finally, Lines¹⁴ Green's-function calculations indicate that χ diverges.

We checked one cycle of our program by hand. We also checked the program by running it for a one-dimensional isotropic system for which exact results are readily available.²⁹ Our computer program required only a change of two cards to convert from a 2D system to a 1D system. As mentioned, our main test of convergence was simply repeatability of results for different random starting configurations of the spins. At low temperatures for 1D systems, the magnetization changed so slowly that it almost appeared to converge to incorrect results. Thus, apparent convergence in one run was necessary but not sufficient to guarantee true convergence. In most of the runs we moved sequentially through the lattice (changing each suc-

cessive spin at random) in order to generate new states. A new state was defined each time a spin was changed by a random amount. The sequential results were little different from the results obtained by choosing a site at random and then making a random change in the direction of the spin at that site. For a small lattice, computer time rather than computer memory was the limiting factor.

The modified Monte Carlo method does have the very great advantage of requiring no new techniques to treat systems with anisotropies and in magnetic fields.

B. Results

Our results are presented in Figs. 3–16. The “error bars” on the curves denote the fluctuations in the results in different subruns. The plotted curves are the averages of the results of several subruns. In order to give a feel for the fluctuations, and at the same time retain some clarity in the plots, error bars are only put on selected graphs. When the convergence was slow we often found it advantageous to let the system “run” a while (in order to settle down) before we started utilizing the results. This was often necessary at low temperatures when the initial random configuration was not a characteristic system for the canonical ensemble at that temperature.

Figures 3 and 4 for the magnetization and energy are fairly easy to understand. At small β or high temperature we expect the spins to be disordered so we should have small magnetization and near zero energy (for no external field, this is the highest energy with our Hamiltonian). For large β or small temperature the spins should be almost ordered (with a preferred axis due to uniaxial anisotropy or magnetic field), thus we should have near saturation magnetization and an energy nearly equal to the lowest energy. At intermediate temperatures, the convergence is slow because the system is undergoing a transition from order to disorder. The slow convergence is indicated by the increase in size of the “error bars” caused by the fluctuations. The large fluctuations in \bar{m} and \bar{u} occur as expected where c_h and χ_T (Figs. 5 and 6) show maxima (although the fluctuations in χ_T and c_h are too large in this region to assign definite values to the maxima or to their location β_c). The variation of the magnetization with anisotropy is also shown in Fig. 4(b). Not surprisingly, the smaller is η (higher anisotropy) the higher the temperature that the magnetization tends to saturate. At low temperatures the energy is independent of the anisotropy. This is expected. The spins are essentially lined up along an axis, and variation of exchange coupling (η) in other directions is not important. The isotropic ($\eta = 1$) series and the spin-wave results, as well as the Monte Carlo results, are plotted in Fig. 3(b).

Note the rather close agreement of appropriate cases. The spin-wave results for the magnetization also appear to show rather close agreement with Monte Carlo results at appropriate temperatures as shown in Fig. 4(b).

The χ_T and c_h curves of Figs. 5(a) and 6(a), although less reliable than the \bar{m} and \bar{u} curves, are perhaps more interesting. Even with anisotropy we might expect that \bar{m} for a finite system should go to zero as $h \rightarrow 0$ (for all temperatures). The reason \bar{m} should go to zero is that $\bar{m} = \bar{m}_{z>0} + \bar{m}_{z<0}$ and by symmetry $\bar{m}_{z>0} = -\bar{m}_{z<0}$. If this actually happened, we would not expect our χ_T (with $h = 0$) to be characteristic of an infinite system. It is certainly true that an exact analytical solution of our model would show $\bar{m}(h \rightarrow 0) = 0$, for any N not finite. However, because there is an energy barrier between being magnetized along z or $-z$, in the computer runs the system appeared to settle in one state of magnetization (for low temperatures) and remain there. In some sense the computer calculations on our model behaves more like a true magnet than analysis might lead us to expect. The largeness of c_h and χ_T at $\beta_c \sim 1.15$ indicates there is an analogy to a phase transition at this temperature. We only see one peak and within the accuracy with which we can clearly identify the peak it is not very close to the Stanley-Kaplan (SK) value of $\beta_{SK} = 2.31$. It is still possible that our β_c would go over to β_{SK} for very weak anisotropies and very large lattices. This would meet the criterion of Lines.¹⁴ However, from our results for \bar{m} , \bar{u} , χ_T , and c_h we could not accurately see any variation of β_c with anisotropy. At low temperatures, we were not able to run to convergence for χ_T as $\eta \rightarrow 1$ and so we could obtain no direct evidence about the SK transition as originally derived for the isotropic case. In Figs. 5(b) and 6(b), spin-wave and series results for χ_T/β and $c_h/(k_B\beta^2)$ are plotted.

Several other results are also obtainable from our calculations. In Figs. 7(a) and 7(b), for $\eta = \frac{1}{2}$, we see that the mean energy per spin is relatively insensitive to the number of spins, whereas the magnetization is somewhat sensitive to number at the higher temperatures. Figure 8 again shows that the mean energy is completely insensitive to anisotropy well below the critical temperature, as we should expect. Figure 9 shows that for $0.1 \leq \eta \leq 0.9$, the rms magnetization is relatively insensitive to anisotropy, particularly above the critical temperature. As $\eta \rightarrow 1$ and $N \rightarrow \infty$, the rms magnetization must go to zero by the Mermin-Wagner theorem. Our results suggest that ($N = \infty$) magnetization may be a very sensitive function of η as $\eta \rightarrow 1$. It is hard to make any firm predictions from the results of Fig. 10, but they are certainly consistent with the idea that χ_T increases with η for $T < T_c$. Figure 11(a) shows that for small magnetizations there

may be appreciable differences between the rms magnetization and the magnetization. The "error" bars on this curve are for the rms magnetization. Figure 11(b) shows that the magnetization varies strongly with field above the Curie temperature but less strongly below, as we should expect. Figure 12 shows the linear behavior of the mean energy as a function of field. Figure 13 is consistent with the idea that χ_T increases as h decreases (at least for $T < T_c$). Figure 14 is a log-log plot of magnetization versus $\beta - 1.15$ for various anisotropies. The plots are certainly consistent with $\bar{m} = K(\beta - \beta_c)^{\beta_1}$ with β_1 not greatly different from the Ising value of 0.125. By placing "error bars" on the plotted points, we have estimated for $\eta = 0.1$ that $\beta_1 \approx 0.09 \pm 0.02$, for $\eta = 0.5$ that $\beta_1 = 0.11 \pm 0.03$, and for $\eta = 0.9$ that $\beta_1 = 0.16 \pm 0.06$. We are not able to predict $\beta_c(\eta)$ (to our accuracy we cannot definitely see a dependence on η). In fact, several combinations of β_c and β_1 give a linear description of our Monte Carlo results on log-log paper. For Figs. 15 and 16 we also chose $\beta_c = 1.15$. Figure 15 shows that our χ_T/β results are consistent with a power-law dependence on $|\beta - \beta_c|$, for $h = 0$, both above and below the critical temperature. We estimate for $T > T_c$ that the slope of the line in Fig. 15(a) has magnitude 1.2 ± 0.3 , and for $T < T_c$ that the slope of the line in Fig. 15(b) has magnitude 1.3 ± 0.5 . Finally, Fig. 16 shows that our \bar{u} results are consistent with a power-law behavior for $T < T_c$. The slope in Fig. 16 is estimated to be 0.2 ± 0.03 . We hesitate to claim that the slopes of Figs. 14–16 ac-

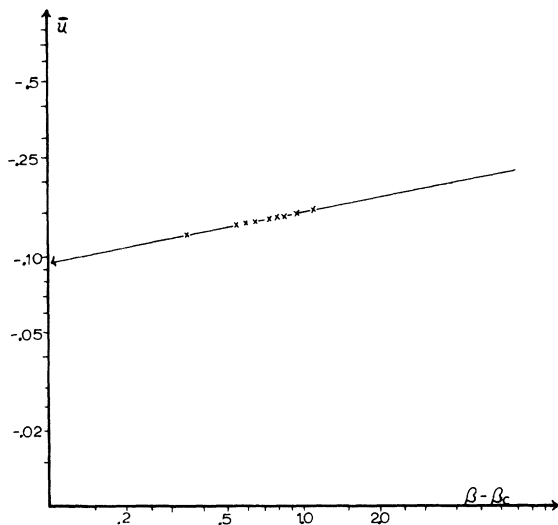


FIG. 16. Mean energy (\bar{u}) vs $\beta - \beta_c$ by Monte Carlo calculation for $\eta = 0.5$, $h = 0$, $N = 100$, and $\beta_c = 1.15$. The slope is about 0.2.

curately predict the values of critical exponents, because the plotted points do not involve very small values of $|(\beta - \beta_c)|/\beta_c$.

VII. CONCLUSIONS

(a) For fairly large anisotropy, at least, \bar{m} and \bar{u} appear to obey a power law below T_c . For \bar{m} , the characteristic exponent (describing the power-law behavior) is not far removed from the Ising value.

(b) $\beta_c < \beta_{SK}$ and the "critical" temperature does not vary much (say more than 50%) with anisotropy when the anisotropy η is perpendicular to the symmetry axis (and η varies from 0.1 to 0.9) in a uniaxial ferromagnet.

(c) We were neither able to confirm nor deny the SK transition. However, some of our results are rather hard to understand unless one believes $\chi_T \rightarrow \infty$ for low temperatures and $\eta \rightarrow 1$. More extensive calculations for the $\eta = 1$ case are also compatible with the SK result.³⁰

(d) The magnetization is relatively insensitive to η for $\eta < 1$ (for low temperature) but may vary rapidly as $\eta \rightarrow 1$. The mean energy is essentially completely insensitive to anisotropy η at low temperature.

(e) If one restricts oneself to fairly large anisotropies and uses temperatures fairly well removed from the critical temperature, then it appears that a lattice of 100 spins is a fair approximation to a lattice with an infinite number of spins as far as calculating static thermodynamic quantities are concerned. The magnetization is more sensitive to number than is the mean energy.

(f) In spin-wave theory, the mean energy and constant-field specific heat are evaluated more accurately than the magnetization and constant-temperature susceptibility. This is because at low temperatures and for weak anisotropies and fields the incipient divergence caused by small ω_k in $1/\omega_k$ is canceled out by an ω_k multiplying factor. It appears that as far as quantities which involve only near-neighbor interactions are concerned, long-short-range order is almost as good as true long-range order (at least as far as the results of spin-wave theory go). Somewhat analogous results appeared to be true for the Monte Carlo calculations.

Finally, we have not discussed the concept of bound magnons because they appear to be of no importance for classical systems.³¹

ACKNOWLEDGMENTS

Professor Walter R. Johnson and Professor Howard A. Blackstead were very helpful in furnishing information needed for writing the computer programs for the UNIVAC-1107.

*Research supported in part by the U. S. Atomic Energy Commission under Contract No. AT(11-1)-427.

†On sabbatical leave (1969-70) from the South Dakota School of Mines and Technology, Rapid City, S. D. 57701.

¹R. J. Birgeneau, H. J. Guggenheim, and G. Shirane, Phys. Rev. B **1**, 2211 (1970).

²M. E. Lines, Phys. Rev. **164**, 736 (1967).

³M. E. Lines, Phys. Letters **24A**, 591 (1967).

⁴M. E. Lines, J. Appl. Phys. **40**, 1352 (1969).

⁵D. J. Breed, K. Gilijamse, and A. R. Miedema, Physica **45**, 205 (1969).

⁶M. E. Lines, J. Phys. Chem. Solids **31**, 101 (1970).

⁷W. Duffy, Jr., D. L. Strandberg, and J. F. Deck, Phys. Rev. **183**, 567 (1969).

⁸M. S. Seehra, Phys. Letters **28A**, 754 (1969).

⁹J. Skalyo, Jr., G. Shirane, and S. A. Friedberg (unpublished).

¹⁰J. Akimitsu, Y. Ishikawa, and Y. Endoh, Solid State Commun. **8**, 87 (1970).

¹¹N. D. Mermin and H. Wagner, Phys. Rev. Letters **17**, 1133 (1966).

¹²D. Jasnow and M. E. Fisher, Phys. Rev. Letters **23**, 286 (1969).

¹³J. Skalyo, G. Shirane, R. J. Birgeneau, and H. J. Guggenheim, Phys. Rev. Letters **23**, 1394 (1969).

¹⁴M. E. Lines (unpublished).

¹⁵H. E. Stanley, Phys. Rev. **158**, 546 (1967).

¹⁶H. E. Stanley and T. A. Kaplan, Phys. Rev. Letters **17**, 913 (1966).

¹⁷M. A. Moore, Phys. Rev. Letters **23**, 861 (1969).

¹⁸D. Jasnow and M. Wortis, Phys. Rev. **176**, 739 (1968).

¹⁹R. E. Watson, M. Blume, and G. H. Vineyard, Phys. Rev. **181**, 811 (1969).

²⁰C. Kittel, in *Introduction to Solid State Physics* (Wiley, New York, 1966), p. 464.

²¹T. H. Berlin and M. Kac, Phys. Rev. **86**, 821 (1952).

²²M. Abramowitz and I. A. Stegun, Natl. Bur. Std. Appl. Math. Series **55**, 591 (1964).

²³H. E. Stanley, Phys. Rev. **158**, 546 (1967).

²⁴N. W. Dalton and D. W. Woods, Proc. Phys. Soc. (London) **90**, 459 (1967).

²⁵Principally the work of D. L. Hofer of the South Dakota School of Mines and Technology.

²⁶M. S. Seehra, Phys. Letters **28A**, 754 (1969).

²⁷N. Metropolis, A. W. Rosenbluth, M. N. Rosenbluth, A. H. Teller, and E. Teller, J. Chem. Phys. **21**, 1087 (1953).

²⁸L. D. Fosdick, *Methods in Computational Physics* (Academic, New York, 1963), Vol. 1, p. 245.

²⁹M. E. Fisher, Am. J. Phys. **32**, 343 (1964).

³⁰R. E. Watson, M. Blume, and G. H. Vineyard, Phys. Rev. B **2**, 684 (1970).

³¹M. Wortis, Phys. Rev. **132**, 85 (1963).

PHYSICAL REVIEW B

VOLUME 3, NUMBER 1

1 JANUARY 1971

High-Field Behavior in the Kondo Effect*

R. A. Weiner

Physics Department, University of California, San Diego, La Jolla, California 92037

and

Physics Department, Carnegie-Mellon University, Pittsburgh, Pennsylvania 15213[†]

and

M. T. Béal-Monod

Physique des Solides, Faculté des Sciences, 91 Orsay, France[‡]

(Received 17 July 1970)

Third-order perturbation-theory calculations of the conduction-electron scattering in dilute magnetic alloys are examined in the regime $\mu_B H \gg kT_K$, T_K the Kondo temperature. The results are compared with the high-field resistivity of dilute CuCr alloys, with an S-matrix calculation of the field dependence of the Hall coefficient, and with the high-field behavior of the thermopower in AuFe alloys. Suggestions are made for systematic studies in the high-field regime.

It has been pointed out that perturbation theory for the *s-d* exchange Hamiltonian converges in two regimes: for high temperatures, $T > T_K$, T_K the Kondo temperature, and also for high fields, $\mu_B H > kT_K$.¹ In this paper we shall investigate the properties of perturbative calculations of the transport properties of dilute magnetic alloy systems in the high-field regime. A third-order perturbation-theory calculation, whose details have been published else-

where,² for the resistivity ρ will be compared with the high-field low-temperature measurements by Daybell and Steyert³ in CuCr, and a similar calculation of the Hall coefficient⁴ R will be compared with More's⁵ results in an S-matrix theory valid at all values of T and H . The high-field behavior of the thermopower⁶ will also be discussed.

An energy average with a weight factor given by the derivative of the Fermi function is required in